Analysis of exosomal circRNAs upon irradiation in pancreatic cancer cell repopulation

Yi-yun Chen
Donghua University
Ming-jie Jiang
Shanghai Jiao Tong University School of Medicine
Zhi-long Chen
Donghua University
Ling Tian (TL09168@hotmail.com)
Shanghai Jiao Tong University School of Medicine

Research article

Keywords: Exosome, circular RNA, cancer repopulation, pancreatic cancer, irradiation, gene expression profiling

Posted Date: August 21st, 2019

DOI: https://doi.org/10.21203/rs.2.13331/v1

Version of Record: A version of this preprint was published on July 29th, 2020. See the published version at https://doi.org/10.1186/s12920-020-00756-3.

Abstract

Background Pancreatic cancer is one of most malignant tumors. However, radiotherapy can lead to tumor recurrence, which is the cause of the residual surviving cells repopulation by some molecular released from dying cells. Exosomes may mediate cell-cell communication and transfer kinds of signals from the dying cells to the surviving cells for stimulating tumor repopulation. Circular RNAs (circRNAs) may be one vital kind of exosomal cargos involving in modulating cancer cell repopulation. Methods Next generation sequencing (NGS) and bioinformatics were performed to analysis and annotate the expression profiles and functions of exosome-derived circRNAs in pancreatic cells during radiation. 4 circRNAs were chosen for qRT-PCR analysis to validate the sequencing. Results A total of 12572 circRNAs were identified, and 3580 circRNAs were annotated in literatures and circBase. There were 196 filtered differentially expressed circRNAs (182 for up-regulated and 14 for down-regulated, fold change >2, p-value <0.05). Gene Ontology (GO) and Kyoto Encyclopedia of Genes and Genomes (KEGG) analyses indicated that regulation of metabolic process and lysine degradation were the main biological processes and pathway enrichment. Conclusions The hsa_circ_002130-hsa_miR_4482-3p-NBN interaction network suggested potential miRNA sponge and target mRNA. Our results provided potential functions of circRNAs to explore molecular mechanisms and therapeutic targets in pancreatic cancer cell repopulation upon irradiation.

Background

Pancreatic cancer is a highly fatal disease, which the incidence is almost the same as the survival rate of patients. According to latest annual statistics[1], 1762450 new cancer cases and 606880 cancer deaths were projected to occur in the United States. Especially, there were 45750 deaths estimated among 56770 cases confirmed in pancreatic cancer, which were with lower incidence but high mortality. Focusing on the global burden of cancer worldwide, the number of new cases and deaths of pancreatic cancer respectively were 458918 and 432242 with 2.5% and 4.5% of its proportion severally[2]. Thus, the treatment of pancreatic cancer is extremely urgent. As known, several treatments are taken for pancreatic cancer, including surgery, chemotherapy, radiotherapy, endoscopic therapy *etc.* Neoadjuvant therapy was also widely used in recent years[3]. Although such kinds of treatments could relieve patients' symptoms, they were limited to reduce the prognosis of patients with pancreatic cancer in 5 years. It has been found that radiotherapy could cause tumor accelerated repopulation, which is known as the main cause of treatment failure[4, 5]. Recently, our team reveled that cancer cell repopulation after radiotherapy were related to the dying cells caused by the treatment, which could inactivate or activated relevant signaling to stimulate the residual surviving cells to fast grow. The related molecules, such as PGE2, microRNAs and other molecules, played as a switch to promote the repopulation[6–8]. Exosomes, one type extracellular vesicle of about 30–150 nm, contain rich cargos such as DNA, mRNA, microRNA (miRNA), long non-coding RNA (lncRNA), and circular RNA (circRNA)[9], which are important regulators of gene expression, especially the post transcription and epigenetic network. Recently, it has been well reported that exosomes might transmit the key factors to the receptor cells, which promote the tumorigenesis and

progression[10, 11]. Thus, further exploring the contents of pancreatic cancer cell-derived exosomes would help to reveal the molecular mechanism of repopulation upon irradiation.

CircRNAs are predominantly in the cytoplasm, which form a covalently closed continuous loop without 5'cap or 3' polyadenylated tail[12]. Therefore, they are more stable than the linear RNA and resistant towards exonucleases. Based on their biogenesis mechanism, different kinds of circRNAs could be characterized to mainly five parts, exonic circRNAs, intronic circRNAs, antisense circRNAs, sense overlapping circRNAs and intergenic circRNAs[13]. And exonic circRNAs were the most detected[14]. Besides, miRNA sponge is one of compelling functions of circRNAs. As endogenous competitive RNAs, circRNAs can compete for miRNAs through MREs (miRNA recognition elements, MREs)[15, 16]. Recently, it was also reported circRNAs could be sorted into exosomes and participate in cancer progression[17]. Especially, exosome-derived circRNAs could promote invasive growth through miRNA sponge in pancreatic cancer[18]. Although sponge miRNAs are partly demonstrated during radiation, the function of circRNAs remains largely unknown.

During the last decades, next generation sequencing (NGS) has been widely used to identify the differentially expression, functional pathways and early diagnosis of pancreatic cancer at genomic, transcriptome and epigenetic level[19, 20]. In this study, we generated RNA sequencing data from 4 types of pancreatic cancer cells (PANC–1, SW1990, BxPC–3, MIAPaCa–2) which were treated with or without irradiation, and identified ~12570 circRNAs. The expression levels of selected differentially expressed circRNAs (DE-circRNAs) were further verified by quantitative real-time reverse transcription PCR (qRT-PCR). GO and KEGG pathway enrichment analysis were then performed to reveal the molecular regulatory networks. A circRNA-miRNA-mRNA network was subsequently constructed to explore their interactions.

Methods

Cell culture

4 pancreatic cancer cells were used for analysis, including PANC–1 (CRL–1469, ATCC), BxPC–3 (CRL–1687, ATCC), SW1990 (CRL–2172, ATCC) and MIA PaCa–2 (CRL–1420, ATCC). Receiving irradiation as an experimental group (group B), while no radiotherapy as a control group (group A). 10 Gy of X-ray radiation was used in experimental group as we reported to induce tumor repopulation before[6, 7]. Cell culture was pretreated to avoid the interference with experimental results, which using 120000 g, 18 h for centrifuging fatal bovine serum[21].

Isolation and identification of exosomes

Differential centrifugation is the most commonly used method for exosome purification. Briefly, low-speed centrifugation and high-speed centrifugation are used alternately to separate vesicular particles of similar size. Centrifugation was performed at 300 g, 2,000 g and 10,000 g to remove the live cells, dead

cells and cell debris, respectively. The crude extract of exosomes was obtained by ultra-high speed centrifugation (>100,000 g), and the operation was repeated twice to remove the contaminated protein for collecting the purified exosome[22].

RNA extraction and purification

Total RNAs from two groups (group A and group B) were extracted and purified using TRIzol reagent (Life Technologies, CA, USA), and then treated with DNase I (Takara, Dalian, China) to eliminate genomic DNA contamination following the manufacturer's instructions. The quantity (ng/ml) and purity (260/280) of total RNAs were determined using a NanoDrop ND–100 (Thermo Fisher Scientific, Waltham, MA, USA). Qualified total RNA was used in the following experiments.

circRNA library construction and sequencing

Total RNA was used for removing rRNAs using Ribo-Zero rRNA Removal Kits (Illumina, USA) following the manufacturer's instructions. RNA libraries were constructed by using rRNA-depleted RNAs with TruSeq Stranded Total RNA Library Prep Kit (Illumina, USA) according to the manufacturer's instructions. Libraries were controlled for quality, and quantified using the BioAnalyzer 2100 system (Agilent Technologies, USA). 10 pM libraries were denatured as single-stranded DNA molecules, captured on Illumina flow cells, amplified in situ as clusters and finally sequenced for 150 cycles on Illumina HiSeq Sequencer according to the manufacturer's instructions.

Sequence mapping and circRNA annotation

Paired-end reads were harvested from Illumina HiSeq 4000 sequencer, and were quality controlled by Q30. After 3' adaptor-trimming, the low quality reads were removed by Cutadapt software (v1.9.3), and the high quality reads were aligned to the hg19 human reference genome with STAR software (v2.5.1b). circRNAs were detected and identified with DCC software (v0.4.4). edgeR software (v3.16.5) was used to normalize the data and perform the differentially expressed circRNA analysis. GO and KEGG analysis were performed for predicting the differentially expressed circRNA-associated genes.

Identification of DE-circRNAs

DE-circRNAs in the two groups were identified using the edgeR software with quasi-likelihood F test (fold change >2 and p-value <0.05). The DE-circRNAs were $\log_2$ transformed, gene mean centred and visualized as a heatmap. Volcano plots were generated using ggplot2 in R (https://cran.r-project.org/web/packages/ggplot2/index.html).

Functional annotation of target miRNAs and prediction of interaction networks

For functional annotation, all host genes of the DE-circRNAs were subjected to GO (http://www.geneontology.org) and KEGG (http://www.genome.jp/kegg/) pathway enrichment analyses using DAVID Bioinformatics Resources (http://david.ncifcrf.gov/home.jsp). The p-value was calculated using a fisher test and corrected by Benjamini & Hochberg adjustment. The prediction of potential circRNA-miRNA binding sites was performed using TargetScan (http://www.targetscan.org) and miRanda (http://www.microrna.org/microrna/home.do). The circRNA-miRNA-mRNA interaction analysis was performed for top 3 expression quantity by using TargetScan, miRanda, Circinteractome (https://circinteractome.nia.nih.gov/) and Circbank (http://www.circbank.cn/). The enrichment score was comprehensive considered to the score from TargetScan and the thermodynamic properties of the binding site from miRanda. The predicted target genes of the DE-circRNAs were further subjected to GO term and KEGG pathway analyses. The gene network analysis was performed using Cytoscape.

qRT-PCR

Total RNA was reverse transcribed using random primers with the PrimeScript RT reagent kit (RR037A, Takara, Dalian, China) according to the manufacturer's protocol. We randomly selected 4 DE-circRNAs, including 3 up-regulated and 1 down-regulated circRNAs. Details of the primer sequences are summarized in Supplementary Table 4. Only primers achieving a single peak in the melting curve were considered proper for qRT-PCR validation. The qRT-PCR was performed using SYBR Premix Ex Taq II (Takara, Dalian, China) on a QuantStudio 6 Flex (Life technologies, USA) according to the manufacturer's instructions. The relative expression of candidate circRNAs was normalized to β-actin and then calculated using the $2^{-\triangle\triangle Ct}$ method. All experiments were repeated in triplicate and presented as the means ±SD.

RNase R treatment

DNase-treated total RNAs were incubated for 1 hr at 37°C with or without RNase R (Epicentre). We used linear RNA FBXW7, GAPDH, β-actin and 18S RNA (which is poly(A)-tailed and must be degraded by RNase R treatment) and circRNA FBXW7 (which is RNase R-resistant and must be non-polyadenylated) as controls.

Western blot

Protein extract was separated by 10% SDS-polyacrylamide gel electrophoresis (SDS-PAGE) and then transferred to a nitrocellulose membrane (Sigma-Aldrich, MO, USA). After blocking for 90 min, membranes were incubated with TSG101 antibody (1:1000; Abcam, UK) at 4°C overnight. Membranes were washed and incubated for 1.5 hr with secondary antibodies (1:5000; Goat Anti-Rabbit IgG (H+L) Dylight 800,

Odyssey, LI-COR, USA). The band intensity was measured using Empiria Studio. GAPDH was used as a loading control.

Statistical analysis

Statistical analyses were performed using GraphPad Prism 7.0 (version 7.0c; GraphPad Software, San Diego, CA, USA). All the data were displayed as the mean ± SEM for triplicate independent measurements. T test was used to assess the differences between experimental groups. Differences with p-value <0.05 were considered statistically significant.

Results

Exosomes characterization and RNA-seq libraries construction

Exosomes secreted by pancreatic cancer cells (PANC–1, SW1990, MIA Paca–2, BxPC–3) which were treated with (group B) or without (group A) irradiation were obtained by ultracentrifugation. Morphology and grain size observation and western blot analysis were used to identify the exosomes. Under transmission electron microscope (TEM), exosomes were irregular spheres ranging of 30–100 nm in diameter (Figure 1A, B). The irradiation group was denser than the control one. Grain size of exosomes was shown at 30–150 nm, which agreed well with the references[9–11]. Accordingly, the concentration of irradiation group was higher than the control one (Figure 1C, D). Western blot was performed to analyze TSG101 (Figure 1E), a common biomarker of exosome[22]. However, there was no expression inside the cells.

To systematically identify circRNAs from exosomes of the pancreatic cancer cells suffering irradiation, approximately 380 million reads for 4 samples were sequenced using quality-controlled total RNA-seq (rRNA depleted). The quality of RNA was shown in Supplementary Table 1. Libraries were controlled for quality and quantified using the BioAnalyzer 2100 system (Agilent Technologies, USA). 10 pM libraries were denatured as single-stranded DNA molecules, captured on Illumina flow cells, amplified in situ as clusters, and finally sequenced for 150 cycles on Illumina HiSeq Sequencer according to the manufacturer's instructions (Supplementary Table 2). More than 86% of 10096 circRNAs were by UCSC hg19 with STAR software (v2.5.1b) (Supplementary Table 3). CircRNAs were detected and identified with DCC software (v0.4.4). EdgeR software (v3.16.5) was used to normalize the data and perform differentially expressed circRNA analysis (Figure 1F). Further bioinformatics analysis would be performed for the differentially expressed circRNA-associated genes.

Expression profiling of circRNAs

12572 cicRNAs were quantitated the expression of circRNAs in whole samples, of which 8992 were novel based on comparison with circBase and published literatures. The expression of the majority of circRNAs

were the exonic circRNAs in all samples, whereas the sense overlapping circRNAs were just taken up a small proportion. Differently, among different expressed circRNAs (DE-circRNAs, fold change >2, p-value <0.05), the intergenic circRNAs were taken up the least (Figure 2A). The details of the newly and known circRNAs in 5 isoforms were shown respectively in Figure 2B. The further proportion rate among 5 isoforms of DE-circRNAs was shown in Supplementary Figure 1A. Among the exonic circRNAs, the mean length of known circRNAs were majorly concentrated on 200–300 nt (254 nt, Figure 2C). On the basis of the expression, known circRNAs were distributed across all chromosomes among the whole circRNAs, while except for chromosome 22 and chromosome Y among novel circRNAs. The distribution of circRNAs across chromosome 1 and 2 was more significant than other chromosomes (Figure 2D). Similarly, the chromosome distribution of DE-circRNAs was also exhibited (Suppementary Figure 1B). Furthermore, the details of expression files of all circRNAs quantitated in our study were presented in Supplementary Data 1 and 2. And the data of chromosomallocation of the DE-circRNAs were also shown in Supplementary Data 3.

Visualization and functiona clustering of DE-circRNAs

circRNA expression levels changed in these exosomes. 196 of DE-circRNAs were identified and shown in heatmap, consisting of 182 up-regulated and 14 down-regulated circRNAs (Figure 3A, fold change >2, p-value <0.05). Especially, all the DE-down-regulated circRNAs were located on the chromosome M. We noted that 174 circRNAs were 6 folds significantly up-regulated, 7 circRNAs were 8 folds significantly up-regulated, and 1 circRNA (hsa_circ_000284) were more than 8 folds significantly up-regulated. Moreover, 12 circRNAs were 6 folds significantly down-regulated, and 2 novel circRNAs (chrM:14131–15754- and chrM: 14131–115754+) were 8 folds significantly down-regulated (Figure 3B). Based on the expression, the volcano plot also revealed the dysregulated circRNAs clustered in red square (Figure 3C).

586 GO terms were significantly enriched for the host genes of the up-regulated circRNAs, which contained biological process (BP), cellular component (CC) and molecular function (MF). As shown in Figure 3D, the top 10 significantly enriched in BP, CC and MF. The genes on the regulation of metabolic process, binding and intracellular were most significant respectively in GO. However, there was no term enriched for the genes of the down-regulated circRNAs. 26 KEGG pathways were associated with the DE-circRNAs. As shown in Figure 3E, the top 10 enriched pathways were highly associated with lysine degradation, phagosome, axon guidance, allograft rejection, HTLV-I infection, endocytosis, Type I diabetes mellitus and Graft-versus-host disease. Furthermore, the details of all terms of GO and KEGG were shown in Supplementary Data 4 and 5.

Experimental validation of circRNA-sequencing

4 circRNAs (hsa_circ_0000419, hsa_circ_0001523,hsa_circ_0000825, and chrM:14131–15754) identified as DE-circRNAs by high-throughput sequencing were randomly selected for validation (Figure 4A). qRT-PCR was performed to detect the expression of these circRNAs in Group A and B, which used for RNA-seq.

We also selected the above mentioned circRNA, circFBXW7, and paired the linear RNA[23], mRNA of common housekeeping genes (β-actin, GAPDH, and 18S RNA) as controls for the RNase R resistance experiment. The results of qRT-PCR revealed that the expression of all linear RNAs (FBXW7, β-actin, GAPDH and 18S RNA) significantly decreased after 1 hr of RNase R digestion (** p-value <0.001). This indicated that circRNAs were resistant to RNase R digestion, whereas linear RNA was sensitive to R treatment (Figure 4B).

Prediction of circRNA-miRNA interaction network

To further clarify the potential roles of circRNAs, we showed most significant circRNAs and expressed in two samples of each group (p-value <0.0001) to construct a circRNA-miRNA interaction network using bioinformatics prediction software. Top 5 significant miRNAs were chosen as the circRNA targets (Figure 5). The circRNA-miRNA interaction analysis for all DE-circRNAs was shown in Supplementary Data 6.

hsa_circ_0002130/hsa_miR_4482–3p/NBN interaction axis

According to the expression quantity of the bioinformatics prediction, 3 top known circRNAs (hsa_circ_0002130, hsa_circ_0000825 and hsa_circ_0005882, p-value <0.001) were chosen to construct the circRNA-miRNA-mRNA interaction networks (Figure 6A), and the newly circRNAs were shown in Supplementary Figure 2. To predict the binding sites of these miRNAs on the 3'UTR of differentially expressed genes, top 5 miRNAs and top 3 genes with the highest binding force were chosen. The most significant circRNA, hsa_circ_0002130, as to further observed the influence of target genes. For example, the irradiation-induced cellular damage includes the modification of DNA bases resulting in DNA strand breaks[24]. Nibrin (NBN) is the gene whose product is associated with DNA double-strand break repair and DNA damage-induced check point activation[25]. As shown, NBN could be regulated by hsa_miR_4482–3p. The predicted binding sites between hsa_circ_0002130, hsa_miR_4482–3p and NBN were demonstrated in Figure 6B. There were two possible binding sites between hsa_miR_4482–3p and NBN. The expression level was shown in Figure 6C. RNase R experiments were shown in the Supplementary Figure 1C. Furthermore, mRNA level of NBN was up-regulated in exosomes during irradiation (Figure 6D). According to TCGA database, the survival curve for NBN was shown in Figure 6E (Log rank p-value = 0.0234). The survival probability of the high expression of NBN was lower than that of the low one.

Discussion

The 5-year prevalence proportion of pancreatic cancer is just around 10.8 per 100000 in China[26], but the delayed detection leads to limited treatment options, poor therapy responses and unfavourable prognosis. Especially, tumor repopulation usually occurs after a lag phase of cancer cytotoxic therapies, such as radiotherapy and chemotherapy, which causes the treatment failure of cancers[4, 6–8]. Our team and others have revealed that tumor repopulation is associated with the chemoradiation-induced dying

tumor cells[6–8]. We would explore how the dying tumor cells stimulate tumor repopulation. Thereinto, one essential question is that what is released from the dying tumor cells and by what means is transferred to the tumor microenvironment, leading to proliferation of the residual surviving tumor cells. Recently, exosomes are known as one kind of important transmitters to cell-cell communication. They are one type of extracellular vesicles, which contain rich cargos, including circRNAs. Several circRNAs such as circ-PDE8A[18], circ-IARS[27] have already been suggested to promote pancreatic cancer progression and might be the potential indicator for early diagnosis and prognostic prediction in pancreatic cancer.

CircRNAs are one new class of RNA regulatory molecules, which explored gradually in recent years. It has been demonstrated that circRNAs were ubiquitous in the transcriptomes of different organisms such as humans, mice, flies worms and other organism[28, 29]. In our study, different circRNAs were produced by selecting different binding sites and existed mainly in exons. 12572 circRNAs were identified, and 3580 circRNAs were annotated as the known circRNAs. We obtained the reads of circRNAs from 5 parts depending on the location of the chromosome, including exonic, intronic, sense overlapping, intergenic and antisense, which were similar to the publication[13]. Most known circRNAs were focus on the exon. And the mean length of the known exonic circRNAs was focus on 200–300 nt. In recent, it has been reported released from nucleus could be influenced by their own length, which indicated that the length of circRNAs might influence its formation[30]. Our study also demonstrated that most of the identified circRNAs (71.52%) are novel. They mainly concentrated on four parts except the exon (Figure 2C). This may be attributed to specific cargos of exosomes, which needs further research. Furthermore, the structure of circRNAs is distinguished from linear RNAs, which have neither a 5'cap or a 3' polyadenylated tail. This unique structure without a poly(A)-tail rendered circRNA highly insensitive to ribonuclease. RNase R, one kind of RNA exonuclease enzyme derived from the RNR superfamily of *E.coli,* can digest almost all linear RNAs, but not circRNAs and lariat RNAs. Based on the concept of circRNAs, RNase-R resistant experiment was applied to validate the reliability of the circRNAs. We showed that circRNAs were more stable than the linear RNAs, further confirming this distinct property. Otherwise, among detecting circRNAs, Ribo-zero was the most frequently used, which ribosomal RNA was adsorbed by probe and then the circRNAs could be kept it in the supernatant. Rencently, Josh et al. show exome capture provided a greater scale against the Ribo-zero, which could detect true circular molecules[31]. Thus, it is worth exploring the new method for obtaining precise data sample in the future.

Expression profiles of circRNAs were further investigated by conducting KEGG and GO analyses, and the potential targets of circRNAs were accordingly predicted. As known, GO unifies genes and gene products of all species, while KEGG pathway analysis reveals the DE-circRNAs participated in several biological pathways. The BP analysis results indicated that the high expression of target genes might be involved in regulation of metabolic process, transcription (DNA-templated), RNA metabolic process, RNA biosynthetic process and nucleic acid-templated transcription. These GO terms might be associated with nucleotide metabolism, which was involved in radiotherapy[32]. Refer to MF, "Binding", "protein methyltransferase activity", "histone methyltransferase activity", "histone methyltransferase activity (H3-K4 specific)" and "histone-lysine N-methyltransferase activity" were important MF-related GO term. As reported, VDR and

p53 in irradiated HEK 293T was related to various biological effects, which mediated gene transcription[33]. Furthermore, aberrant methylation could lead to dysregulation of related transcription-factor genes, which might be closely bound up to irradiation[34, 35]. Moreover, KEGG analysis indicated that the lysine degradation was the most enriched pathway, which was consistent with the results of GO analysis. Lysine degradation mainly participated in the control of gene expression and transcription. These findings indicated the cargos in exosomes could regulate different pathway and biological processes concerning cell proliferation and irradiation. However, further experimental verification is still needed, especially onto tumor repopulation owing to radiotherapy.

In the previous studies, circRNAs were served as one of most important molecular sponges of miRNAs, which could decrease expression of proteins[36]. According to our results, numerous miRNA binding sites were predicted by Circinteractome, Circbank, Miranda and TargetScan, which revealed circRNAs could interact with miRNAs. Based on bioinformatics, circRNA-miRNA-mRNA regulatory network was constructed to clarify the interactions between molecules. As shown in Figure 6A, the hsa_circ_0002130/hsa_miR_4482–3p/NBN interaction axis was involved in the regulatory network. NBN gene encoded protein is a member of the MRE11/RAD50 double-strand break repair complex. Several studies confirmed the crucial roles of NBN are involved in DNA double-strand break repair and DNA damage-induced checkpoint activation[37]. Furthermore, we showed that the level of hsa_circ_0002130 was also up-regulated during irradiation, consistent with the expression pattern of NBN. Given the potential binding sites among hsa_circ_0002130/hsa_miR_4482–3p/NBN, we propose that hsa_circ_0002130 may promote the expression of NBN through the absorption of hsa-miR–4482–3p. More remarkably, some circRNAs were also shown to be translated into proteins[38, 39]. Thus, the underlying mechanisms still needed further investigations.

In recent years, several studies identified the expression profiles of circRNAs in pancreatic cancer. Few studies have focuses on the interaction of circRNAs and miRNAs in exosomes from pancreatic cancer during irradiation. Here, circRNA profiles of exosome-derived circRNAs were shown. And the top 5 putative target miRNAs for DE-circRNAs were identified in pancreatic cancer during irradiation. The construction of a circRNA-miRNA-mRNA interaction network will provide a better understanding of the complex regulatory relationships and mechanisms of irradiation resistant.

Nevertheless, there are still several drawbacks inherent to our study. The small sample size was for RNA-seq, which samples from the patients were hard for us to collect. Therefore, the influence from the patients should be further validated. On the other hand, even if we believe that they worked, we did not perform further experiments to confirm the regulatory relationship among circRNAs, miRNAs and mRNAs, as well as other functions of circRNAs.

Conclusions

We hereinabove first identified and annotated 12572 circRNAs in the exosomes of human pancreatic cancer cells upon irradiation using RNA-seq analysis. Most of these circRNAs were composed of exons.

Some circRNAs were significantly changed during irradiation treatment. Of them, the DE-circRNAs associated with methylation, which was in accord with the signaling pathways. 4 circRNAs were chosen to verify the reliability of RNA-sequencing by using a series of biological experiments. Most of them are consistent with the expectation, but more research on the reliability of results is also needed. Furthermore, construction of the circRNA-miRNA-mRNA interaction network provided a line of inquiry to understand of the relationship of different molecules. We demonstrated that hsa_circ_0002130 could target NBN by combing with the hsa_miR_4482–3p. Based on TCGA database, high expression of NBN revealed a worse survival. This indicated that hsa_circ_0002130 may play an important role in pancreatic cancer during radiotherapy.

Abbreviations

circRNAs: circular RNAs

NGS: next generation sequencing

qRT-PCR: quantitative real-time reverse transcription PCR

miRNA: microRNA

lncRNA: long non-coding RNA

MREs: miRNA recognition elements

GO: gene ontology

KEGG: kyotoencyclopedia of genes and genomes

DE-circRNAs: differentially expressed circRNAs

TEM: transmission electron microscope

BP: biological process

CC: cellular component

MF: molecular function

Declarations

Ethics approval and consent to participate

Not applicable.

Consent for publication

Not applicable.

Availability of data and materials

RNA-Seq data has been submitted to GEO database; accession GSE132678while it remains in private status: ybkzeiuqjpixhkd. All other relevant data is available within the manuscript or its accompanying supplementary material.

Competing interests

The authors declare that they have no competing interests.

Funding

This research was supported by the grants of the National Natural Science Foundation of China (No. 81773073), and Natural Science Foundation of Shanghai (No. 16ZR1427500). The funding bodies had no role in the design of the study, collection, the interpretation of data and in writing the manuscript.

Authors' contributions

YC and MJ performed the experiments, analyzes the data and wrote the manuscript. LT designed the protocols and revised the manuscript. ZC provided some helpful supports. All authors have read and approved the manuscript.

Acknowledgements

We many thank for the funds of National Natural Science Foundation of China, and Natural Science Foundation of Shanghai.

References

[1] Siegel RL, Miller KD, Jemal A. Cancer statistics, 2019. CA Cancer J Clin. 2019; doi: 10.3322/caac.21551.

[2] Bray F, Ferlay J, Soerjomataram I, Siegel RL, Torre LA, Jemal A. Global cancer statistics 2018: GLOBOCAN estimates of incidence and mortality worldwide for 36 cancers in 185 countries. CA Cancer J Clin. 2018; doi: 10.3322/caac.21492.

[3] Strobel O, Neoptolemos J, Jager D, Buchler MW. Optimizing the outcomes of pancreatic cancer surgery. Nat Rev Clin Oncol. 2019; doi: 10.1038/s41571–018–0112–1.

[4] Kim JJ, Tannock IF. Repopulation of cancer cells during therapy: an important cause of treatment failure. Nat Rev Cancer. 2005; doi: 10.1038/nrc1650.

[5] Bentzen SM, Atasoy BM, Daley FM, Dische S, Richman PI, Saunders MI, Trott KR, Wilson GD. Epidermal growth factor receptor expression in pretreatment biopsies from head and neck squamous cell carcinoma as a predictive factor for a benefit from accelerated radiation therapy in a randomized controlled trial. J Clin Oncol. 2005; doi: 10.1200/JCO.2005.06.411.

[6] Fang C, Dai CY, Mei Z, Jiang MJ, Gu DN, Huang Q, Tian L. microRNA–193a stimulates pancreatic cancer cell repopulation and metastasis through modulating TGF-β2/TGF-βRIII signalings. J Exp Clin Cancer Res. 2018; doi: 10.1186/s13046–018–0697–3.

[7] Huang Q, Li F, Liu X, W. Li,Shi W, Liu FF, O'Sullivan B, He Z, Peng Y, Tan AC, Zhou L, Shen J, Han G, Wang XJ, Thorburn J, Thorburn A, Jimeno A, Raben D, Bedford JS, Li CY. Caspase 3-mediated stimulation of tumor cell repopulation during cancer radiotherapy. Nat Med. 2011; doi: 10.1038/nm.2385.

[8] Ma J, Cheng J, Gong Y, Tian L, Huang Q. Downregulation of Wnt signaling by sonic hedgehog activation promotes repopulation of human tumor cell lines. Dis Model Mech. 2015; doi: 10.1242/dmm.018887.

[9] van Niel G, D'Angelo G, Raposo G. Shedding light on the cell biology of extracellular vesicles. Nat Rev Mol Cell Biol. 2018; doi: 10.1038/nrm.2017.125.

[10] Pavlyukov MS, Yu H, Bastola S, Minata M, Shender VO, Lee Y, Zhang S, Wang J, Komarova S, Wang J, Yamaguchi S, Alsheikh HA, Shi J, Chen D, Mohyeldin A, Kim SH, Shin YJ, Anufrieva K, Evtushenko EG, Antipova NV, Arapidi GP, Govorun V, Pestov NB, Shakhparonov MI, Lee LJ, Nam DH, Nakano I. Apoptotic cell-derived extracellular vesicles promote malignancy of glioblastoma via intercellular transfer of splicing factors. Cancer Cell. 2018; doi: 10.1016/j.ccell.2018.05.012.

[11] Becker A, Thakur BK, Weiss JM, Kim HS, Peinado H, Lyden D. Extracellular vesicles in cancer: cell-to-cell mediators of metastasis. Cancer Cell. 2016; doi: 10.1016/j.ccell.2016.10.009.

[12] Vicens Q, Westhof E. Biogenesis of circular RNAs. Cell. 2014; doi: 10.1016/j.cell.2014.09.005.

[13] Memczak S, Jens M, Elefsinioti A, Torti F, Krueger J, Rybak A, Maier L, Mackowiak SD, Gregersen LH, Munschauer M, Loewer A, Ziebold U, Landthaler M, Kocks C, le Noble F, Rajewsky N. Circular RNAs are a large class of animal RNAs with regulatory potency. Nature. 2013; doi: 10.1038/nature11928.

[14] Zheng Q, Bao C, Guo W, Li S, Chen J, Chen B, Luo Y, Lyu D, Li Y, Shi G, Liang L, Gu J, He X, Huang S. Circular RNA profiling reveals an abundant circHIPK3 that regulates cell growth by sponging multiple miRNAs. Nat Commun. 2016; doi: 10.1038/ncomms11215.

[15] Hansen TB, Jensen T, Clausen BH, Bramsen JB, Finsen B, Damgaard CK, Kjems J. Natural RNA circles function as efficient microRNA sponges. Nature. 2013; doi: 10.1038/nature11993.

[16] Bezzi M, Guarnerio J, Pandolfi PP. A circular twist on microRNA regulation. Cell Res. 2017; doi: 10.1038/cr.2017.136.

[17] Zhang H, Zhu L, Bai M, Liu Y, Zhan Y, Deng T, Yang H, Sun W, Wang X, Zhu K, Fan Q, Li J, Ying G, Ba Y. Exosomal circRNA derived from gastric tumor promotes white adipose browning by targeting the miR–133/PRDM16 pathway. Int J Cancer. 2019; doi: 10.1002/ijc.31977.

[18] Li Z, Yanfang W, Li J, Jiang P, Peng T, Chen K, Zhao X, Zhang Y, Zhen P, Zhu J, Li X. Tumor-released exosomal circular RNA PDE8A promotes invasive growth via the miR–338/MACC1/MET pathway in pancreatic cancer. Cancer Lett. 2018; doi: 10.1016/j.canlet.2018.04.035.

[19] Jones S, Zhang X, Parsons DW, Lin JC, Leary RJ, Angenendt P, Mankoo P, Carter H, Kamiyama H, Jimeno A, Hong SM, Fu B, Lin MT, Calhoun ES, Kamiyama M, Walter K, Nikolskaya T, Nikolsky Y, Hartigan J, Smith DR, Hidalgo M, Leach SD, Klein AP, Jaffee EM, Goggins M, Maitra A, Iacobuzio-Donahue C, Eshleman JR, Kern SE, Hruban RH, Karchin R, Papadopoulos N, Parmigiani G, Vogelstein B, Velculescu VE, Kinzler KW. Core signaling pathways in human pancreatic cancers revealed by global genomic analyses. Science. 2008; doi: 10.1126/science.1164368.

[20] Ziller MJ, Gu H, Müller F, Donaghey J, Tsai LT, Kohlbacher O, De Jager PL, Rosen ED, Bennett DA, Bernstein BE, Gnirke A, Meissner A. Charting a dynamic DNA methylation landscape of the human genome. Nature. 2013; doi: 10.1038/nature12433.

[21] Shelke GV, Lässer C, Gho YS, Lötvall J. Importance of exosome depletion protocols to eliminate functional and RNA-containing extracellular vesicles from fetal bovine serum. J Extracell Vesicles. 2014; doi: 10.3402/jev.v3.24783.

[22] Greening DW, Xu R, Ji H, Tauro BJ, Simpson RJ. A protocol for exosome isolation and characterization: evaluation of ultracentrifugation, density-gradient separation, and immunoaffinity capture methods. Methods Mol Biol. 2015; doi: 10.1007/978–1–4939–2550–6_15.

[23] Yang Y, Gao X, Zhang M, Yan S, Sun C, Xiao F, Huang N, Yang X, Zhao K, Zhou H, Huang S, Xie B, Zhang N. Novel role of FBXW7 circular RNA in repressing glioma tumorigenesis. J Natl Cancer Inst. 2018; doi: 10.1093/jnci/djx166.

[24] Baskar R, Lee KA, Yeo R, Yeoh KW. Cancer and radiation therapy: current advances and future directions. Int J Med Sci. 2012; doi: 10.7150/ijms.3635.

[25] Pennisi R, Antoccia A, Leone S, Ascenzi P, di Masi A. Hsp90α regulates ATM and NBN functions in sensing and repair of DNA double-strand breaks. FEBS J. 2017; doi: 10.1111/febs.14145.

[26] Zheng R, Zeng H, Zhang S, Chen T, Chen W. National estimates of cancer prevalence in China, 2011. Cancer Lett. 2016; doi: 10.1016/j.canlet.2015.10.003.

[27] Li J, Li Z, Jiang P, Peng M, Zhang X, Chen K, Liu H, Bi H, Liu X, Li X. Circular RNA IARS (circ-IARS) secreted by pancreatic cancer cells and located within exosomes regulates endothelial monolayer permeability to promote tumor metastasis. J Exp Clin Cancer Res. 2018; doi: 10.1186/s13046–018–0822–3.

[28] Arnaiz E, Sole C, Manterola L, Iparraguirre L, Otaegui D, Lawrie CH. CircRNAs and cancer: biomarkers and master regulators. Semin Cancer Biol. 2018; doi: 10.1016/j.semcancer.2018.12.002.

[29] Qian L, Yu S, Chen Z, Meng Z, Huang S, Wang P. The emerging role of circRNAs and their clinical significance in human cancers. Biochim Biophys Acta Rev Cancer. 2018; doi: 10.1016/j.bbcan.2018.06.002.

[30] Huang C, Liang D, Tatomer DC, Wilusz JE. A length-dependent evolutionarily conserved pathway controls nuclear export of circular RNAs. Genes Dev. 2018; doi: 10.1101/gad.314856.118.

[31] Vo JN, Cieslik M, Zhang Y, Shukla S, Xiao L, Zhang Y, Wu YM, Dhanasekaran SM, Engelke CG, Cao X, Robinson DR, Nesvizhskii AI, Chinnaiyan AM. The landscape of circular RNA in cancer. Cell. 2019; doi: 10.1016/j.cell.2018.12.021.

[32] Gunda V, Souchek J, Abrego J, Shukla SK, Goode GD, Vernucci E, Dasgupta A, Chaika NV, King RJ, Li S, Wang S, Yu F, Bessho T, Lin C, Singh PK. MUC1-Mediated metabolic alterations regulate response to radiotherapy in pancreatic cancer. Clin Cancer Res. 2017; doi: 10.1158/1078–0432.CCR–17–1151.

[33] Pemsel A, Rumpf S, Roemer K, Heyne K, Vogt T, Reichrath J. Tandem affinity purification and nano HPLC-ESI-MS/MS reveal binding of vitamin D receptor to p53 and other new interaction partners in HEK 293T cells. Anticancer Res. 2018; doi: 10.21873/anticanres.12341.

[34] Daino K, Nishimura M, Imaoka T, Takabatake M, Morioka T, Nishimura Y, Shimada Y, Kakinuma S. Epigenetic dysregulation of key developmental genes in radiation-induced rat mammary carcinomas. Int J Cancer. 2018; 10.1002/ijc.31309.

[35] Kejík Z, Jakubek M, Kaplánek R, Králová J, Mikula I, Martásek P, Král V. Epigenetic agents in combined anticancer therapy. Future Med Chem. 2018; doi: 10.4155/fmc–2017–0203.

[36] Du WW, Zhang C, Yang W, Yong T, Awan FM, Yang BB. Identifying and characterizing circRNA-protein interaction. Theranostics. 2017; doi: 10.7150/thno.21299.

[37] Gatei M, Young D, Cerosaletti KM, Desai-Mehta A, Spring K, Kozlov S, Lavin MF, Gatti RA, Concannon P, Khanna K. ATM-dependent phosphorylation of nibrin in response to radiation exposure. Nat Genet. 2000; doi: 10.1038/75508.

[38] Yang Y, Fan X, Mao M, Song X, Wu P, Zhang Y, Jin Y, Yang Y, Chen LL, Wang Y, Wong CC, Xiao X, Wang Z. Extensive translation of circular RNAs driven by N^6-methyladenosine. Cell Res. doi: 10.1038/cr.2017.31.

[39] Legnini I, Di Timoteo G, Rossi F, Morlando M, Briganti F, Sthandier O, Fatica A, Santini T, Andronache A, Wade M, Laneve P, Rajewsky N, Bozzoni I. Circ-ZNF609 is a circular RNA that can be translated and functions in myogenesis. Mol Cell. 2017; doi: 10.1016/j.molcel.2017.02.017.

Figures

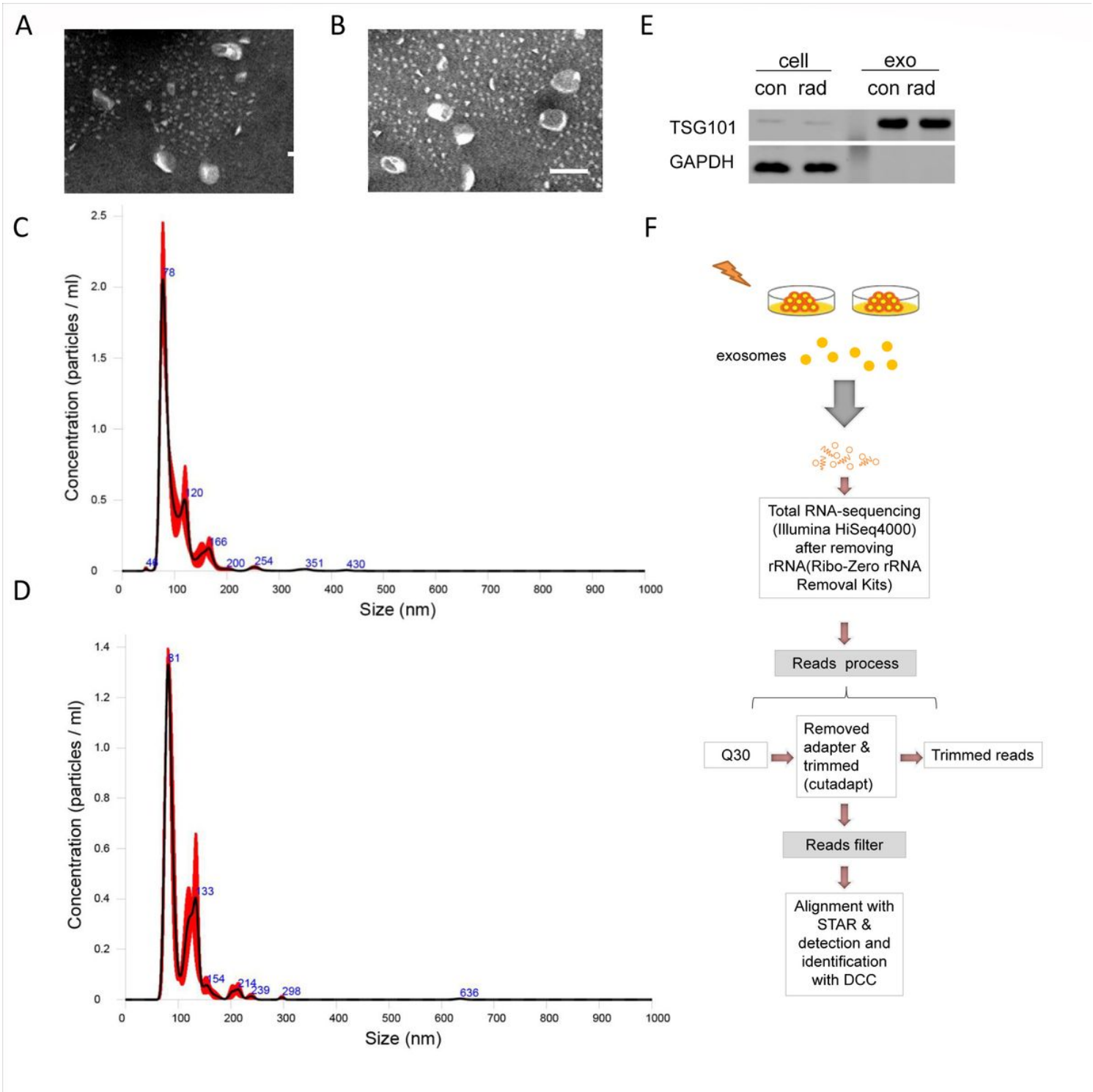

Figure 1

Exosomes characterization and RNA-seq libraries construction. (A, B) Representative TEM image of exosomes in samples. Negative staining was used to enhance the view of membrane structures (bar=100 nm). (C, D) Representative grain-size graph of exosomes in samples. (E) Representative western blot images of the exosomes and cells. (F) Overview of the comprehensive computational scheme for systematic identification of circRNAs in samples.

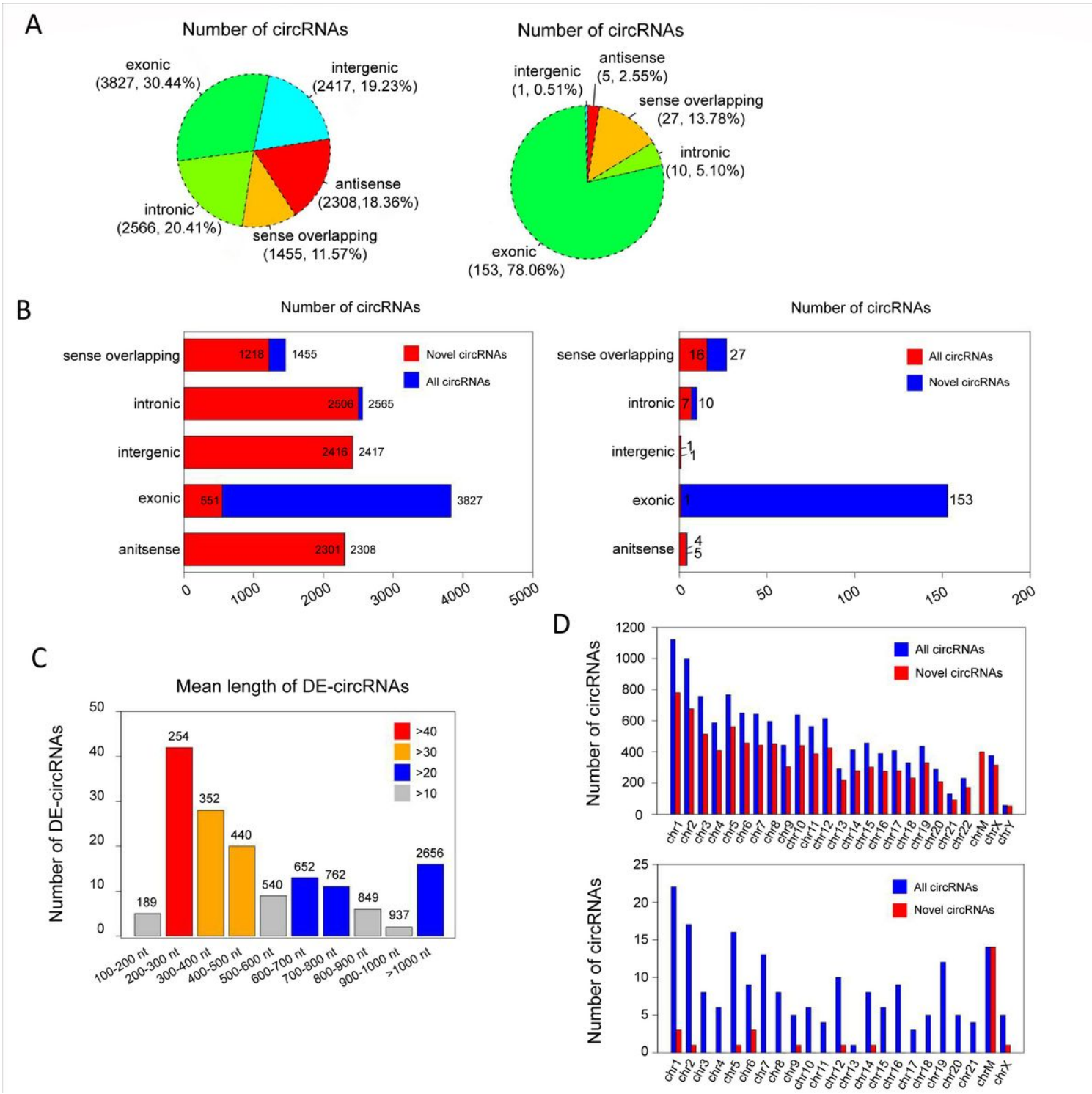

Figure 2

Expression patterns of circular RNAs. (A) The proportion of 5 isoforms of all predicted and differentially expressed (DE) circRNAs. (B) The further distribution of novel circRNAs among all predicted and DE-circRNAs. (C) The mean length of the exonic circRNAs among the known DE-circRNAs. (D) The chromosomal distribution of novel circRNAs among all predicted and DE-circRNAs.

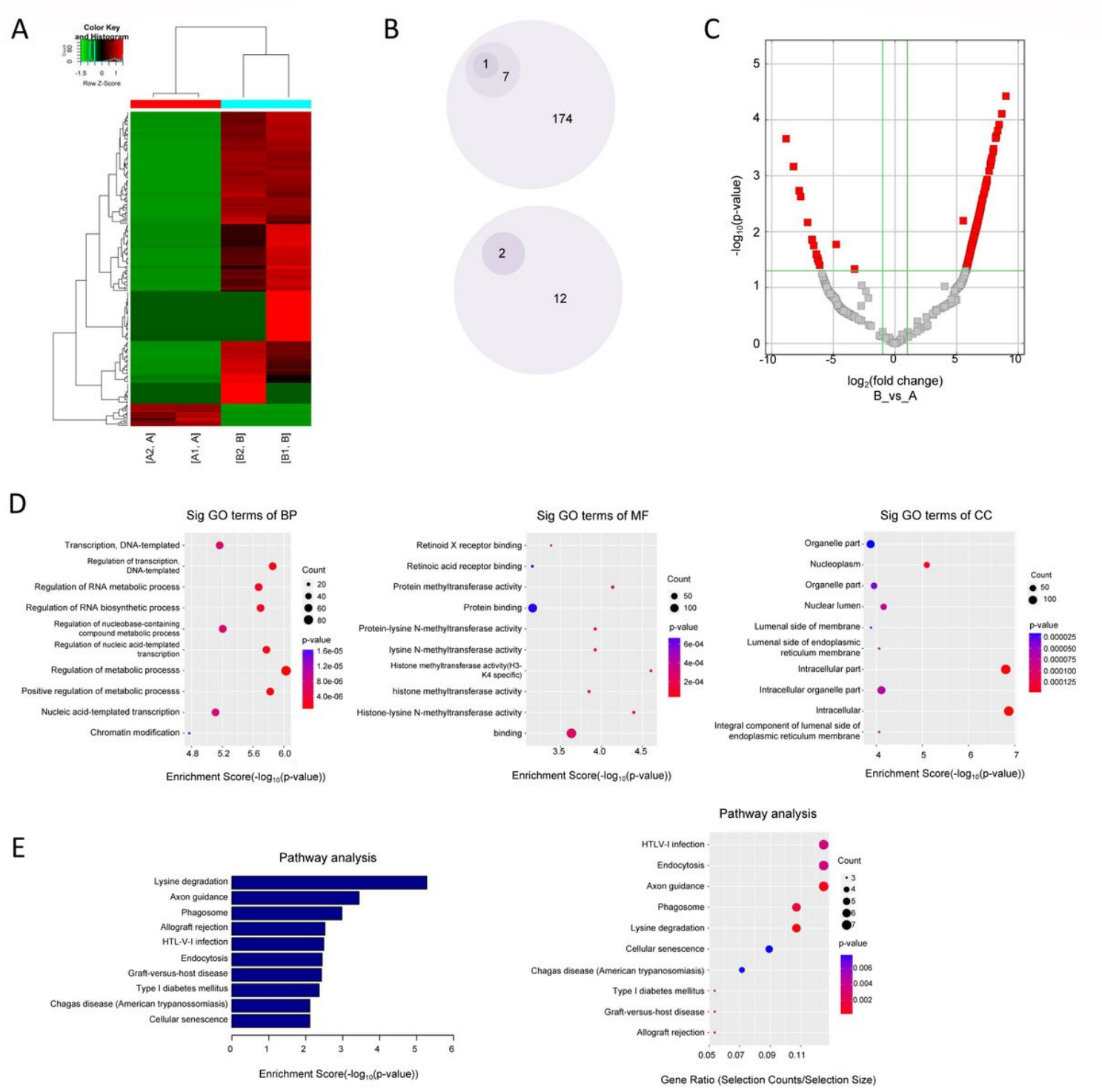

Figure 3

Visualization and functiona clustering of DE-circRNAs. (A) Heatmap of the DE-circRNAs between group A and group B. (B) Bullet graph of the DE-circRNAs between two groups. (C) Volcano plot of the DE-circRNAs. The vertical lines correspond to fold-change, and the horizontal lines to p-value. Red rectangles represent DE-circRNAs (|foldchange| >2.0 and p <0.05). Top 10 items of GO and KEGG enrichment of DE-circRNAs were represented in (D, E).

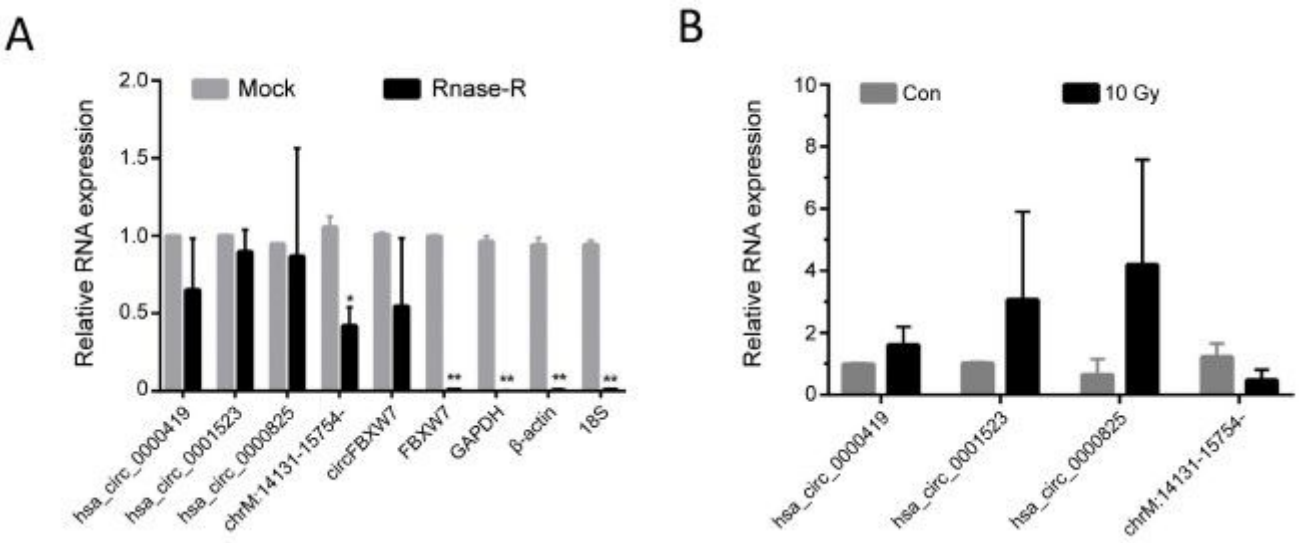

Figure 4

Validation of the circRNA-sequencing results. (A) Expression levels of hsa_ circ_0000419, hsa_circ_0001523, hsa_circ_0000825, and chrM: 14131-15754 in the irradiation group (group B) with that in the non-irradiation group (group A). The results of quantitative real-time PCR (qRT-PCR) were evaluated by 2-△△CT method. Results were represented as means ± standard deviation (SD). *p-value <0.05. (B) CircRNAs were resistant to RNase R digestion, whereas the linear RNAs were sensitive to RNase R digestion. 4 circRNAs were examined, which were qualified in expression level. And FBXW7, GAPDH, β-actin, and 18S RNA were used as negative controls and known circRNA FBXW7 was used as a positive control. The results of quantitative Real-time PCR (qRT-PCR) were evaluated by 2-△CT method. Results were represented as means ± standard deviation (SD) *p-value <0.05, ** p-value <0.001.

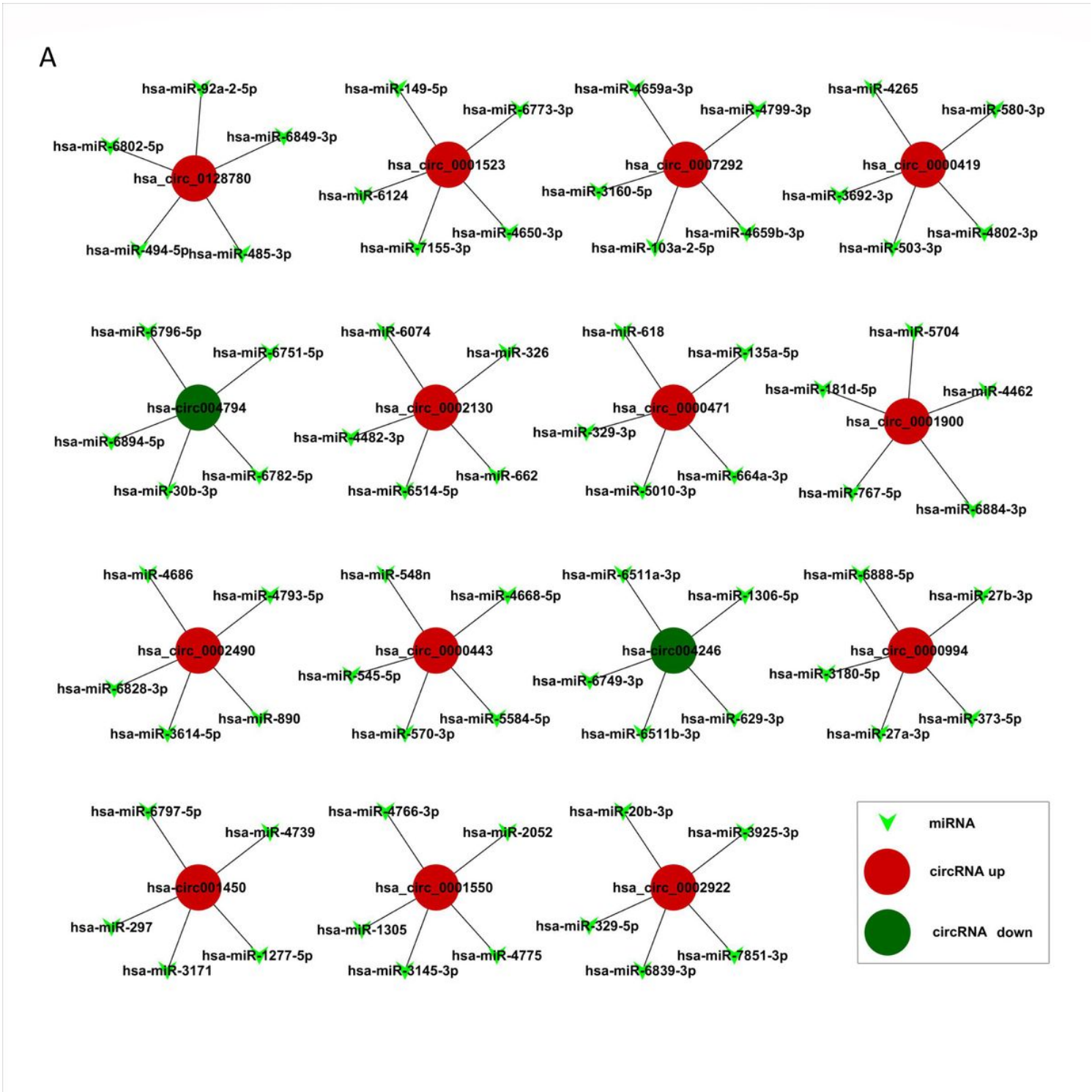

Figure 5

circRNA-miRNA network analysis. The top 15 significantly expressed circRNAs and top 5 predicted miRNAs were selected to generate a network map. The circRNA-miRNA network was constructed using bioinformatics online programs (TargetScan and miRBase). The red circle indicated the up-regulated circRNAs and the green ones indicated the down-regulated ones.

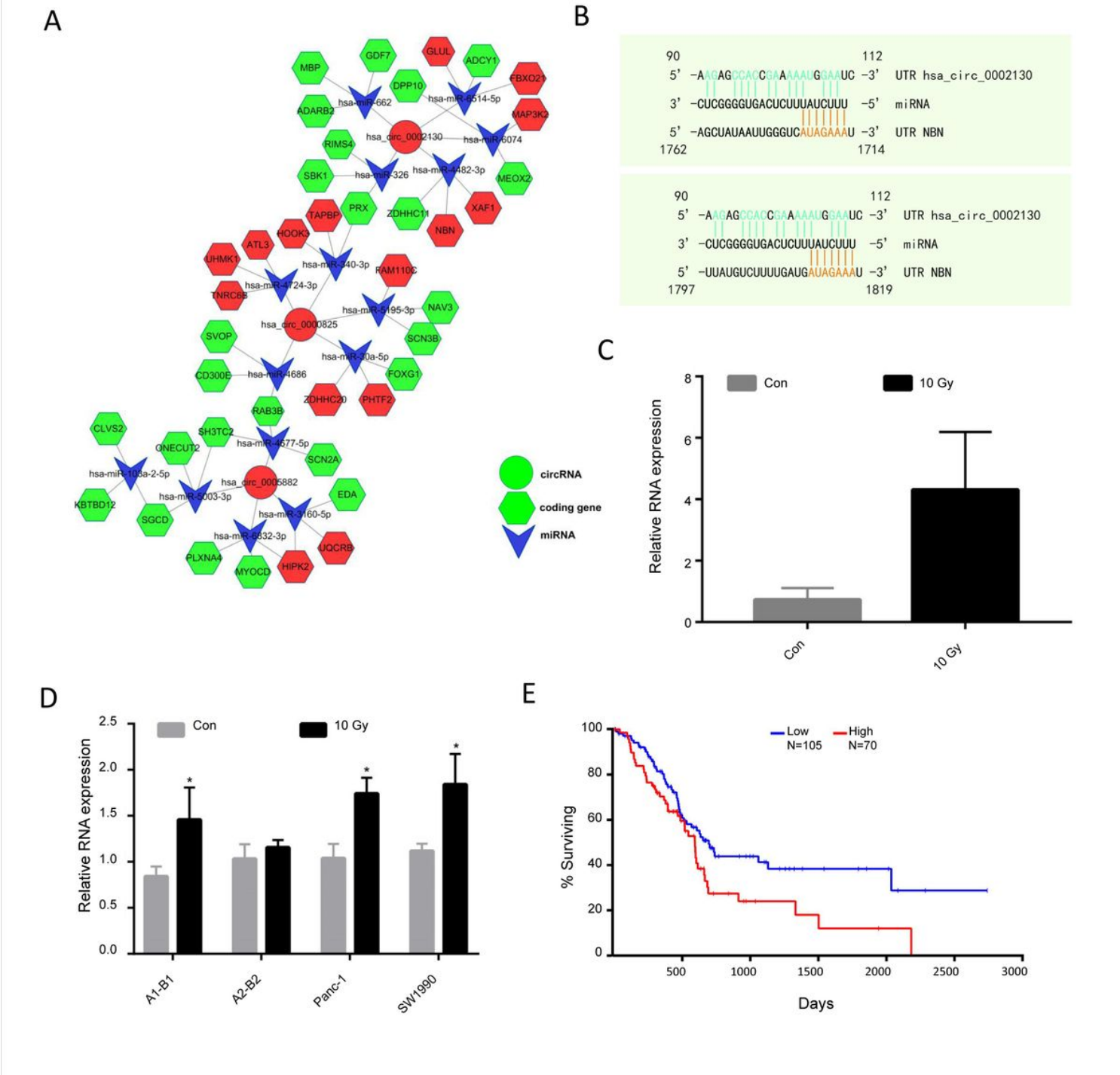

Figure 6

Hsa_circ_0002130-hsa_miR_4482-3p-NBN interaction axis. (A) The predicted circRNA-miRNA-mRNA interaction network was predicted using bioinformatics online programs (Circinteractome, Circbank, TargetScan, and miRBase). The red circle indicates the up-regulated circRNAs, the green indicates the down-regulated ones, the arrow and the hexagon indicate miRNAs and target genes respectively. (B) The predicted binding sites between hsa_circ_0002130 and hsa_miR_4482-3p were exhibited. (C) The expression of hsa_circ_0002130 in samples were examined by qRT-PCR. (D) The expression of NBN was

determined by qRT-PCR in samples of sequencing; PANC-1 and SW1990. *p-value <0.05 and data indicated the mean ±SD. (E) The survival data from TCGA (Log rank p-value=0.0234).

Supplementary Files

This is a list of supplementary files associated with this preprint. Click to download.

- supplement1.xlsx
- supplement1.xls
- supplement2.docx
- supplement4.xlsx
- supplement5.xlsx
- supplement6.xlsx
- supplement7.fa
- supplement8.tif
- supplement9.tif